ACS APPLIED MATERIALS & INTERFACES

Research Article

www.acsami.org

Direct Writing of Three-Dimensional Macroporous Photonic Crystals on Pressure-Responsive Shape Memory Polymers

Yin Fang,[†,∥] Yongliang Ni,[‡,∥] Sin-Yen Leo,[†] Bingchen Wang,[†] Vito Basile,[§] Curtis Taylor,*[,‡] and Peng Jiang*[,†]

[†]Department of Chemical Engineering, University of Florida, Gainesville, Florida 32611, United States

[‡]Department of Mechanical and Aerospace Engineering, University of Florida, Gainesville, Florida 32611, United States

[§]ITIA-CNR, Industrial Technologies and Automation Institute, National Council of Research, Via Bassini, 15, 20133 Milano, Italy

Supporting Information

ABSTRACT: Here we report a single-step direct writing technology for making three-dimensional (3D) macroporous photonic crystal patterns on a new type of pressure-responsive shape memory polymer (SMP). This approach integrates two disparate fields that do not typically intersect: the well-established templating nanofabrication and shape memory materials. Periodic arrays of polymer macropores templated from self-assembled colloidal crystals are squeezed into disordered arrays in an unusual shape memory "cold" programming process. The recovery of the original macroporous photonic crystal lattices can be triggered by direct writing at ambient conditions using both macroscopic and nanoscopic tools, like a pencil or a nanoindenter. Interestingly, this shape memory disorder−order transition is reversible and the photonic crystal patterns can be erased and regenerated hundreds of times, promising the making of reconfigurable/rewritable nanooptical devices. Quantitative insights into the shape memory recovery of collapsed macropores induced by the lateral shear stresses in direct writing are gained through fundamental investigations on important process parameters, including the tip material, the critical pressure and writing speed for triggering the recovery of the deformed macropores, and the minimal feature size that can be directly written on the SMP membranes. Besides straightforward applications in photonic crystal devices, these smart mechanochromic SMPs that are sensitive to various mechanical stresses could render important technological applications ranging from chromogenic stress and impact sensors to rewritable high-density optical data storage media.

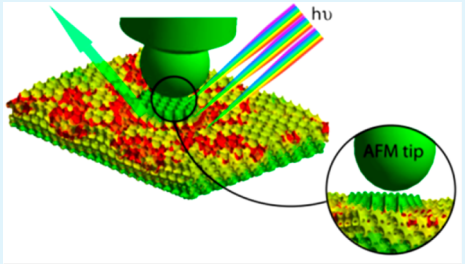

KEYWORDS: *shape memory polymers, nanoindentation, photonic crystals, direct writing, mechanochromic*

1. INTRODUCTION

Three-dimensional printing (or additive manufacturing) has attracted great recent interest, as it enables rapid manufacturing and prototyping of 3D objects with arbitrary shapes and/or geometries.[1−4] In 3D printing, successive layers of materials (e.g., polymers, ceramics, and metal alloys) are laid down under computer control through processes like inkjet printing, extrusion, and sintering. Beyond conventional manufacture of macroscopic objects (e.g., customized shoes, automobile parts, and even guns), 3D printing has also been extensively exploited for fabricating microscopic devices with unique optical, electrical, magnetic, and biological properties.[5−7] One preeminent example is the direct writing of 3D ordered photonic crystals with desired crystal structures and pre-engineered defects.[8−14] Photonic crystals are periodic dielectric structures with a forbidden photonic band gap (PBG) for electromagnetic waves.[15] As 3D photonic crystals with full PBGs can manipulate photons in a similar fashion as semiconductors do electrons, they provide enormous opportunities in controlling the flow of light in microscopic volumes for a plethora of applications ranging from all-optical integrated circuits and quantum information processing to low-threshold lasers and lossless waveguides.[15,16] To fabricate photonic crystals possessing optical and near-infrared (NIR) PBGs, the lattice constant of the artificial crystal must have dimensions on the submicrometer scale.[15,17] Unfortunately, this length scale is formidably challenging for direct-writing-based 3D printing technologies, especially considering the overflow of the ink materials (e.g., photopolymers) in the layer-by-layer deposition process.[4]

Here we report a single-step direct writing technology for reversibly printing 3D macroporous photonic crystal patterns (both macroscopic and nanoscopic) with submicrometer-scale lattice spacing on a new type of pressure-responsive shape memory polymer. This technology integrates scientific principles drawn from two disparate fields: the well-established templating nanofabrication[18−20] and shape memory materials.[21−23] Compared with conventional 3D printing, which needs to address the resolution issue in generating the intrinsic 3D submicrometer-scale microstructures, the current approach utilizes colloidal crystal-based templating nanofabrication in defining the final

Received: August 5, 2015
Accepted: October 8, 2015
Published: October 8, 2015

DOI: 10.1021/acsami.5b07220
ACS Appl. Mater. Interfaces 2015, 7, 23650−23659

photonic crystal lattice parameters.[24,25] Self-assembled colloidal crystals have been widely used as structural templates in fabricating macroporous photonic crystals with periodic arrays of air cavities embedded in the matrix material (e.g., polymer, metal, and semiconductor).[19,25−29] The stringent submicrometer-scale lattice spacing requirement for making visible- and NIR-active 3D photonic crystals can be easily satisfied by controlling the size of the templating colloidal particles.[28] Another major merit of the current technology is the employment of new pressure-sensitive SMPs that enable the direct writing of arbitrary 3D macroporous photonic crystal patterns on the polymer surface in a single step.[30,31] Shape memory polymers are a class of smart materials that can recover their "memorized" permanent shapes triggered by various external stimuli, such as heat, light, solvent, and electromagnetic field.[22,23,32−41] Shape memory (SM) effects in traditional SMPs are usually achieved in three steps: programming, storage, and recovery.[33] In programming, a SMP sample is mechanically deformed from its permanent shape to a temporary configuration by heating the sample above a specific transition temperature (T_{trans}), such as the polymer glass transition temperature (T_g). The temporary shape is then "frozen" in the polymer by cooling the deformed sample below T_{trans}. Recovery to the permanent shape, which is caused by entropy elasticity,[33] can finally be triggered by applying different stimuli, such as reheating the sample above T_{trans} or exposing it to ultraviolet radiation. Although thermoresponsive SMPs have been utilized in making tunable 3D colloidal photonic crystals and 2D diffractive gratings,[42−49] the heat-demanding SM programming and recovery steps impede the ultimate performance and applications of the SMP-enabled microoptical devices.

2. EXPERIMENTAL SECTION

2.1. Templating Nanofabrication of Macroporous SMP Photonic Crystal Membranes. Monodispersed silica microspheres with diameter ranging from 200 to 400 nm were synthesized using the standard Stöber method.[50] The as-synthesized silica microspheres were purified in 200-proof ethanol by using multiple centrifugation and redispersion cycles (at least 5 times). The purified silica particles were then self-assembled on glass microslides to form hexagonally close-packed colloidal single crystals using the well-established convective self-assembly technology.[51] The thickness of the resulting colloidal crystal was controlled to ∼5 μm by adjusting the particle volume fraction of the silica microsphere−ethanol suspension to ∼1.0%. A double-sided adhesive tape (∼1 mm thick) was used as a spacer to separate the glass microslide with the self-assembled silica colloidal crystal on its surface from another bare glass microslide. A viscous oligomer mixture containing 1.5 g of polyethylene glycol (600) diacrylate (SR610, Sartomer, T_g ≈ −42 °C, MW 742, refractive index 1.468), 0.5 g of ethoxylated (20) trimethylolpropane triacrylate (SR415, Sartomer, T_g ≈ −40 °C, MW 1176, refractive index 1.470), and 0.016 g Darocur 1173 photoinitiator (2-hydroxy-2-methyl-1-phenyl-1-propanone, BASF) was injected between the two glass microslides to fill up the gap. The sample became nearly transparent due to the refractive index matching between the oligomer mixture and the silica microspheres. The oligomers were then photopolymerized by exposing the sample to ultraviolet radiation for 4 s using a pulsed UV curing system (RC 742, xenon). The solidified sample was finally soaked in a 1 vol % hydrofluoric acid aqueous solution for 4 h and then rinsed with deionized water. After blow-drying with compressed air, free-standing macroporous SMP membranes resulted.

2.2. Directly Printing and Hand-Writing 3D Macroscopic Photonic Crystal Patterns on Templated Macroporous SMP Membranes. We prepared 2 × 2 cm^2 macroporous SMP membranes as "writing pads" for directly printing and hand-writing 3D photonic crystal patterns on them. Commercial rubber stamps with relief patterns purchased from Office Depot were pressed gently for 2 s on the SMP "writing pads" to print colorful inverted patterns on the macroporous membranes. To directly write 3D photonic crystal features, a homemade writing tool was made by wrapping a pencil with Handi-wrap plastic film. An iridescent "UF" pattern with vivid colors was then directly written on the SMP "writing pad". The colorful patterns can be erased by immersing the SMP membranes in deionized water and then drying out of water. Through thorough investigation, our results showed that the SMP "writing pads" can be reused hundreds of times without apparent degradation in rewritability.

2.3. Directly Writing 3D Photonic Crystal Micropatterns by Atomic Force Microscope (AFM). A MFP-3D atomic force microscope (Asylum Research, CA) was used for writing microscopic patterns on SMP membranes. Both the dedicated MFP-3D Nano-Indenter module (flexure, k = 3814 N/m) and the AFM cantilever-based configuration were used with a 1 mm (sapphire, E = 350 GPa) and a 20 μm (borosilicate, E = 62.8 GPa, nominal k ≈ 42 N/m, length = 125 μm, CP-NCH-BSG cantilever from sQUBE Inc., Bickenbach, Germany) diameter spherical tip, respectively. The minimum force and the displacement resolution of the NanoIndenter module are less than 3 μN and 1 nm, respectively. The resolutions of the cantilever-based configuration are less than 6 nN and 0.1 nm. The writing forces for both configurations were controlled by closed-loop control of the set-point voltage, which defines the amount of the contact force maintained during writing. The MicroAngelo software routine (Asylum Research) was used to program writing parameters including set point voltage, speed, feature geometry, etc.

2.4. Sample Characterization. SEM imaging was carried out on a FEI Nova NanoSEM 430. A thin layer of gold was sputtered onto the samples prior to imaging. Amplitude-modulation atomic force microscopy (AM-AFM) was performed uing the MFP-3D AFM with a Nanosensor PPP-NCHR probe (tip radius of <10 nm). All AFM images were processed using the Scanning Probe Imaging Processor (SPIP, Image Metrology Inc., Horsholm, Denmark) software. Normal-incidence optical reflection spectra were obtained using an Ocean Optics HR4000 high-resolution fiber optic vis−NIR spectrometer with a reflection probe (R600-7) and a tungsten halogen light source (LS-1). Absolute reflectivity was obtained as the ratio of the sample spectrum and a reference spectrum, which was the optical density obtained from an aluminum-sputtered (1000 nm thickness) silicon wafer.

2.5. Scalar Wave Approximation (SWA) Optical Modeling. The scalar wave theory developed for periodic dielectric structures was implemented to model the normal-incidence optical reflection spectra from macroporous SMP photonic crystal membranes.[52] In the SWA theory, Maxwell's equations are solved for a periodic dielectric medium assuming that one may neglect diffraction from all but one set of crystalline planes. In the current work, only the (111) crystalline planes of a face-centered cubic crystal were considered in the modeling. The SWA simulation contained no adjustable parameters, as the size of the macropores and the crystal thickness were experimentally determined from SEM images, and the refractive indices of the SMP copolymers were known.

3. RESULTS AND DISCUSSION

3.1. Concept of Direct Writing of 3D Photonic Crystals on Macroporous SMP Membranes. We have recently discovered a new type of stimuli-responsive shape memory polymer that enables unusual "cold" programming (i.e., the deformation from the permanent shape to the temporary configuration occurs at room temperature) and instantaneous shape recovery at ambient conditions triggered by applying a static contact pressure or exposing the polymer to various organic vapors (e.g., acetone and toluene).[30,31] These new SMPs are composed of photocured copolymers of ethoxylated (20) trimethylolpropane triacrylate (ETPTA 20) and polyethylene glycol (600) diacrylate (PEGDA 600) oligomers with varying volumetric ratios from 1:1 to 1:6. Figure 1 shows an exemplary pressure-induced SM recovery process using an ETPTA 20-*co*-PEGDA 600 copolymer with a 1:3 volumetric ratio. The relief

DOI: 10.1021/acsami.5b07220
ACS Appl. Mater. Interfaces 2015, 7, 23650−23659

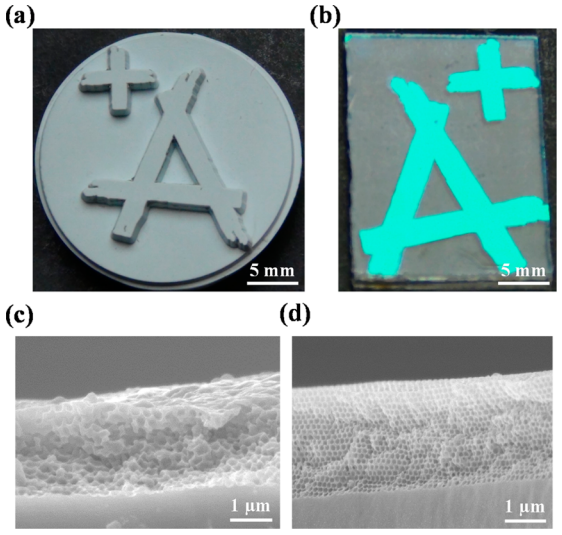

Figure 1. (a) Photograph of a rubber stamp with a "$^{+}$A" relief pattern on its surface. (b) Photograph of an iridescent "A^{+}" pattern printed on a translucent macroporous SMP membrane with 280 nm macropores. (c) Cross-sectional SEM image showing the translucent region in (b). (d) Cross-sectional SEM image showing the iridescent region in (b).

"$^{+}$A" pattern on the surface of a commercial rubber stamp (Figure 1a) was inversely printed on a translucent SMP membrane with collapsed macropores (temporary configuration, Figure 1c). The SM recovery of the permanent, 3D ordered macroporous arrays (Figure 1d), which were templated from self-assembled colloidal crystals consisting of 280 nm silica microspheres, led to the iridescent structural colors of the printed "A^{+}" pattern in Figure 1b. To explain this counterintuitive pressure-induced recovery of collapsed macropores, we proposed a SM recovery mechanism triggered by an adhesive pull-off force caused by the attractive van der Waals interactions between the rubber stamp and the pressure-responsive SMP membrane.[30] However, this new recovery mechanism is far from being thoroughly investigated and verified. Here we explore a new direct writing technology for inscribing arbitrary 3D photonic crystal patterns on the above pressure-responsive SMP membranes. In sharp contrast to the vertical pull-off force in our previous static printing process (Figure 1), the lateral shear stress plays a critical role in this dynamic approach.

The scheme in Figure 2 illustrates the basic concept of the new direct writing technology for making 3D ordered photonic crystal patterns on a macroporous SMP membrane with collapsed macropores. The self-standing SMP membranes were produced by templating nanofabrication using convectively self-assembled silica colloidal crystals as structural template.[53] In this process, ETPTA 20 and PEGDA 600 oligomer mixtures were first photopolymerized in the interstitials of 3D ordered silica particle arrays. The cross-linked polymer chains in the 3D inversely ordered polymer matrix were primarily in an energetically favorable, stress-free configuration, denoting the permanent state of the SMPs. After removal of the templating silica microspheres in a hydrofluoric acid aqueous solution and drying the SMP membrane out of water, the originally ordered macropores were surprisingly collapsed, resulting in the translucent appearance of the film (see Figure 1b). Our previous studies showed that strong capillary pressure induced by water evaporation deformed the elastic macropores (T_g of the copolymers ≪ room temperature) into disordered arrays in

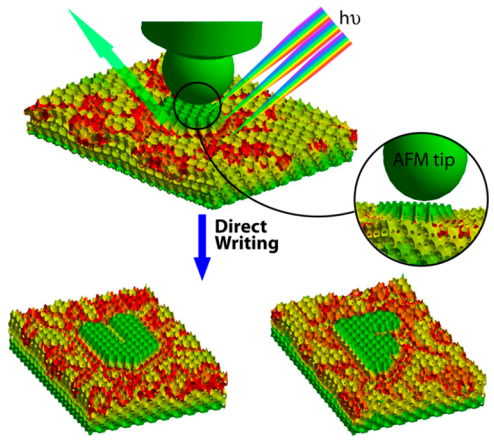

Figure 2. Schematic illustration showing the direct writing of microscopic 3D photonic crystal patterns (letters "U" and "F") on a macroporous SMP membrane with collapsed macropores using an AFM tip.

this "cold" programming process (i.e., the deformation of ordered macropores occurred at ambient conditions as compared to traditional "hot" programming steps),[30] storing excess stresses in the squeezed, temporarily configured polymer chains. The recovery of the permanent, stress-free state (i.e., 3D ordered macroporous arrays) can be triggered by direct writing using either macroscopic or microscopic writing tools like a conventional pen or an atomic force microscope tip. As the SM recovery is confined only to the regions underneath the writing tool and the recovered feature size is mainly determined by the sharpness of the writing tip, we can generate nanoscopic photonic crystal patterns, like the letters "U" and "F" in Figure 2 (representing the abbreviations for University of Florida), using a sharp AFM tip. In addition to inducing the above disorder-to-order transition, the direct writing process can also pop up the deformed macropores underneath the tip, making the recovered photonic crystal patterns protrude out of an otherwise disordered background.

3.2. Direct Writing of Macroscopic Photonic Crystal Patterns. We started to demonstrate the direct writing of 3D photonic crystal patterns on pressure-responsive SMP membranes using macroscopic writing tools like a conventional fountain pen (without ink). However, the direct writing-induced SM recovery of collapsed macropores was not as straightforward as that exhibited by static printing.[30] Although well-defined writing marks were left underneath the stainless steel tip of the fountain pen, these marks were pale-colored, indicating an incomplete macropore recovery process. Our extensive experiments revealed that the tip material plays a determining role in triggering SM macropore recovery. Hard materials, like metals, graphite (pencil cores), and hard plastics (e.g., polystyrene), were found inefficient in generating colorful patterns; while soft materials, such as low density polyethylene (LDPE) and polydimethylsiloxane (PDMS) with different elastic moduli (synthesized by controlling the mixing ratio of the two precursors of Sylgard 184 PDMS), were much easier in inducing a complete macropore recovery. We speculate that soft materials could induce stronger van der Waals interactions between the writing tip and the SMP membrane than harder tips and thus lead to larger pull-off force for popping up the deformed macropores. Video S1 in the Supporting Information (am5b07220_si_002.avi) shows a direct writing process using a LDPE-wrapped pencil as the writing tool. Iridescent features with the same dimension

DOI: 10.1021/acsami.5b07220
ACS Appl. Mater. Interfaces 2015, 7, 23650−23659

as the writing tip immediately showed up following the movement of the tip. Figure 3a displays a greenish "UF" pattern written on a translucent macroporous SMP copolymer membrane templated from 300 nm silica microspheres. The typical cross-sectional scanning electron microscope (SEM) image in Figure 3b reveals that the macropores in the noniridescent regions in Figure 3a are disordered and the surface of the deformed membrane is quite rough. By contrast, the macropores in the recovered iridescent regions are 3D highly ordered and the film surface is much smoother (Figure 3c). The average thickness of the macroporous layer changes from 2.77 ± 0.26 μm for the disordered array to 4.56 ± 0.04 μm for the recovered photonic crystal, indicating a 65% expansion of the deformed macropores. Importantly, the directly written photonic crystal patterns stored at ambient conditions are stable for a long period of time. The batches of samples prepared 8 months ago still maintain their vivid iridescent colors and well-defined patterns. No spontaneous recovery of the deformed macropores was observed at ambient conditions.

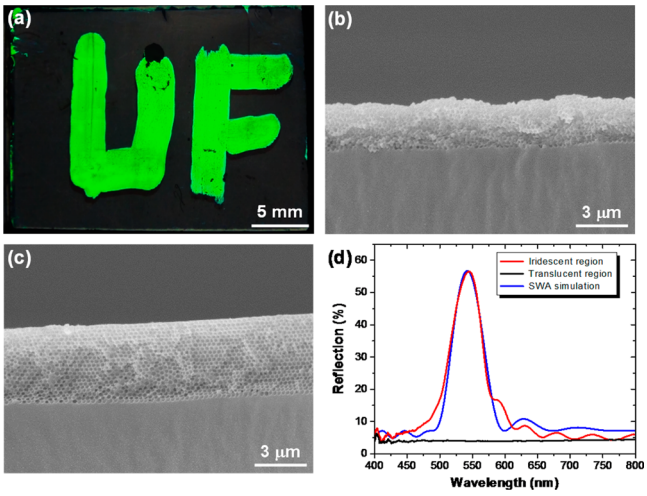

Figure 3. (a) Photograph of a green-colored, handwritten "UF" pattern on a translucent macroporous SMP membrane with collapsed 300 nm macropores. (b) Typical cross-sectional SEM image of the translucent region in (a). (c) Typical cross-sectional SEM image of the iridescent region in (a). (d) Normal-incidence optical reflection spectra obtained from the iridescent and the translucent regions of the sample in (a). The simulated spectrum using a SWA model is also shown to compare with the experimental results.

The different optical appearances of the translucent and the iridescent regions in Figure 3a can be quantitatively characterized by comparing their normal-incidence optical reflection spectra (Figure 3d). No apparent Bragg diffraction peaks are shown in the spectrum corresponding to the translucent region, while a distinct optical stop band located at ~543 nm with well-defined Fabry–Perot fringes is present in the spectrum obtained from the iridescent region. Importantly, the experimental spectrum matches well with the simulated spectrum using a scalar-wave approximation model which assumes a perfect face-centered cubic (fcc) crystalline lattice with its (111) planes normal to the incident light.[52] This good match demonstrates the high crystalline quality of the writing-recovered photonic crystals.

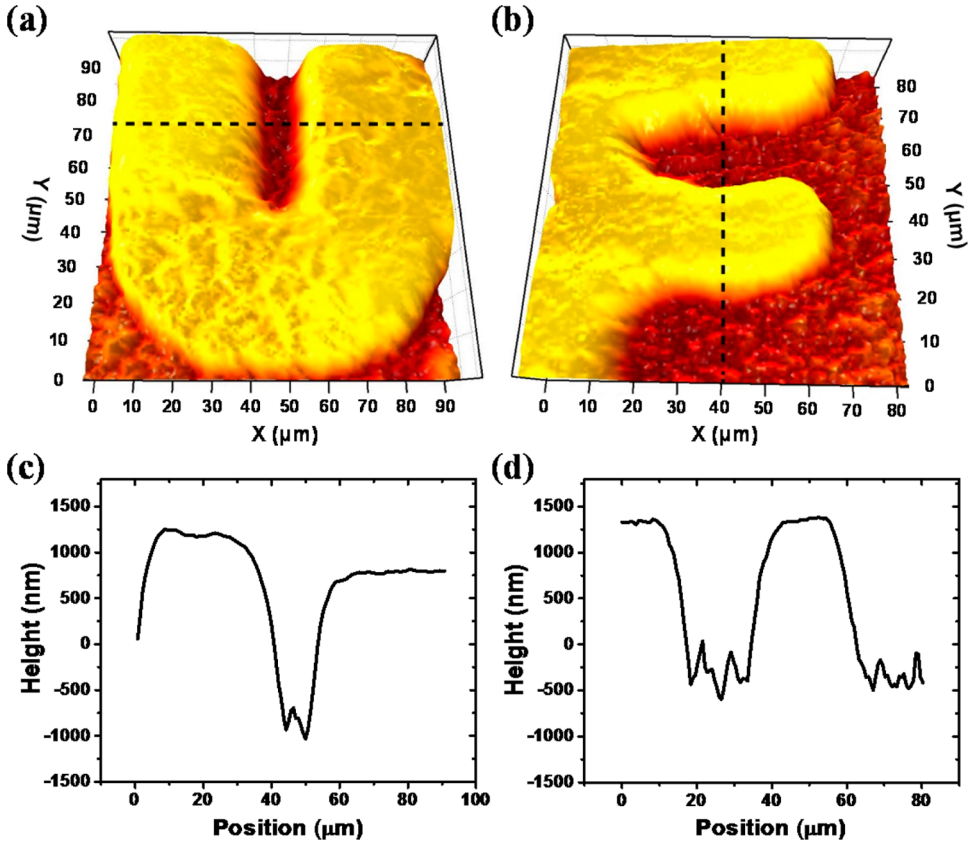

Figure 4. (a) AFM image of a micropattern "U" directly written on a macroporous SMP membrane using a 1 mm diameter sapphire spherical tip. (b) AFM image of a micropattern "F". (c) Height profile scanned across the dashed line in (a). (d) Height profile scanned across the dashed line in (b).

DOI: 10.1021/acsami.5b07220
ACS Appl. Mater. Interfaces 2015, 7, 23650–23659

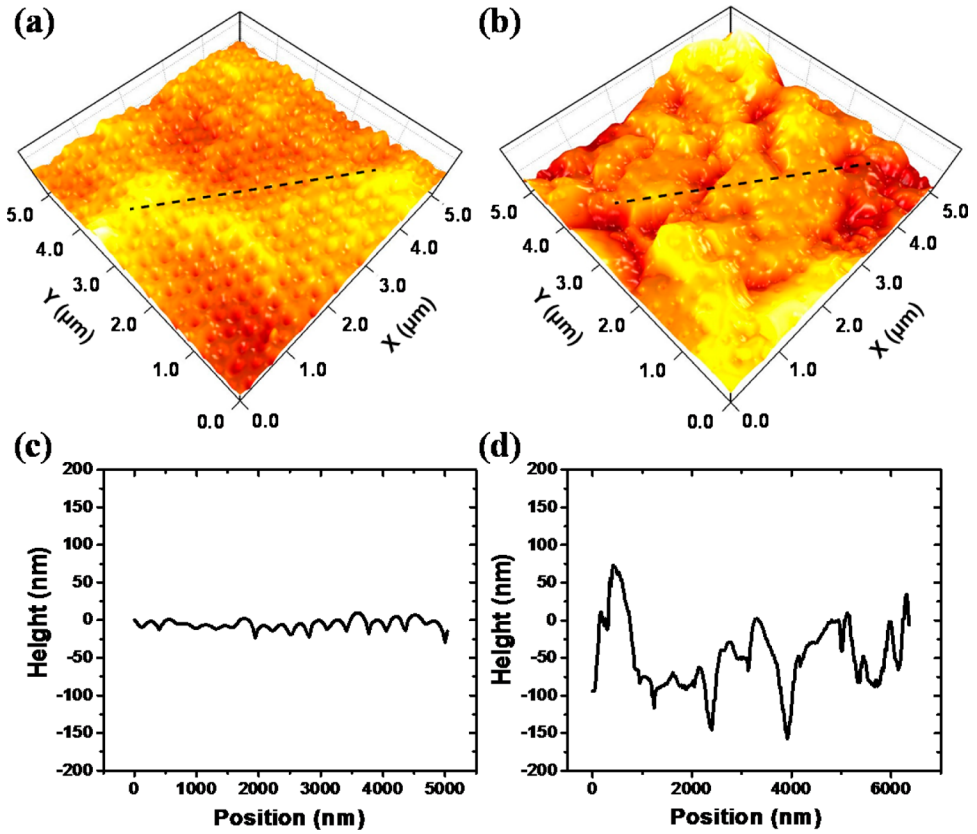

Figure 5. (a) Higher resolution AFM image of a recovered area on the micropatterned letter "U" in Figure 4a. (b) Higher resolution AFM image of an unpatterned area. (c) Height profile scanned across the dashed line in (a). (d) Height profile scanned across the dashed line in (b).

Moreover, the direct writing process is reversible. As shown by video S2 in the Supporting Information (am5b07220_si_003.a-vi), the prewritten photonic crystal patterns can be entirely erased by drying the SMP membrane out of water. New photonic crystal features can then be written on the regenerated translucent film. This rewriting process can be repeatedly done without apparent degradation in the chromogenic response of the SMP membranes. Figure S1a and Figure S1b show the normal-incidence optical reflection spectra obtained from a macroporous SMP membrane under nine cycles of writing and erasing processes. A comparison of the absolute reflection amplitudes of the diffraction peaks in Figure S1a and the amplitudes taken at 550 nm wavelength in Figure S1b confirms the good reversibility of the reconfiguration processes.

3.3. Direct Writing of Nanoscopic Photonic Crystal Patterns. In addition to macroscopic writing tools, atomic force microscopy was used to explore the capability in directly writing micro/nano-scale photonic crystal features under well-controlled conditions. Figure 4a and Figure 4b shows AFM images of the designed "U" and "F" micropatterns written on a SMP copolymer membrane with 300 nm macropores using a 1 mm diameter sapphire spherical tip. Both letters were written with 140 μN contact force at a lateral writing speed of 5 μm/s. Each letter was written within a $100 \times 100\ \mu m^2$ region. As illustrated by the corresponding depth profiles in Figure 4c and Figure 4d, the letters protrude out from the rough membrane surface to a height of ~2 μm, and the minimum line width achieved by using the blunt tip is approximately 30 μm. The raised letters indicate that the SMP surface underwent a vertical transformation during the direct writing process, agreeing with the apparent thickness increase of the macroporous layer (~1.8 μm) revealed by SEM (see Figure 3b and Figure 3c). Optical microscopy images (not shown here) illustrate that only the micropatterned areas reflect brilliant green light. A further observation of the SMP surface topography by higher resolution AFM imaging (Figure 5) shows not only that the patterned areas are much smoother than the unpatterned areas (Figure 5c and Figure 5cd) but also that the ordered arrangement of the macropores only appears on the patterned areas (Figure 5a and Figure 5b). The root-mean-square (rms) linear profile roughness (R_q) of the patterned and unpatterned regions is 5.53 ± 0.75 μm and 50.51 ± 8.93 μm, respectively. The combination of the above observations including the ordered surface macropore structure supports that the reflective "UF" micropatterns are periodic arrays of recovered macropores.

3.4. Critical Contact Pressure Inducing SM Recovery. To determine the critical contact pressure that can trigger the recovery of the deformed macropores during direct writing, a series of microscopic lines were written with decreasing force by controlling the set-point voltage applied to the AFM flexure. Figure 6a shows an optical microscope image (in transmission mode) of six lines written with 13.8, 27.7, 138, 277, 830, and 1380 μN force (from left to right, corresponding to 0.005, 0.01, 0.05, 0.1, 0.3, and 0.5 V set-point voltage). The tip writing speed was held constant at 1 μm/s. In addition to the apparent difference in line width as revealed by the optical microscope image, other characteristics of the written lines were identified by AFM images (Figure 6b–g) and the corresponding depth profiles (Figure 6h–m). The line widths determined by both AFM and optical microscope images decrease from ~60 μm for the maximum force (1380 μN) to ~25 μm for the minimal force (13.8 μN), while the heights of the protruding lines are nearly constant at

DOI: 10.1021/acsami.5b07220
ACS Appl. Mater. Interfaces 2015, 7, 23650–23659

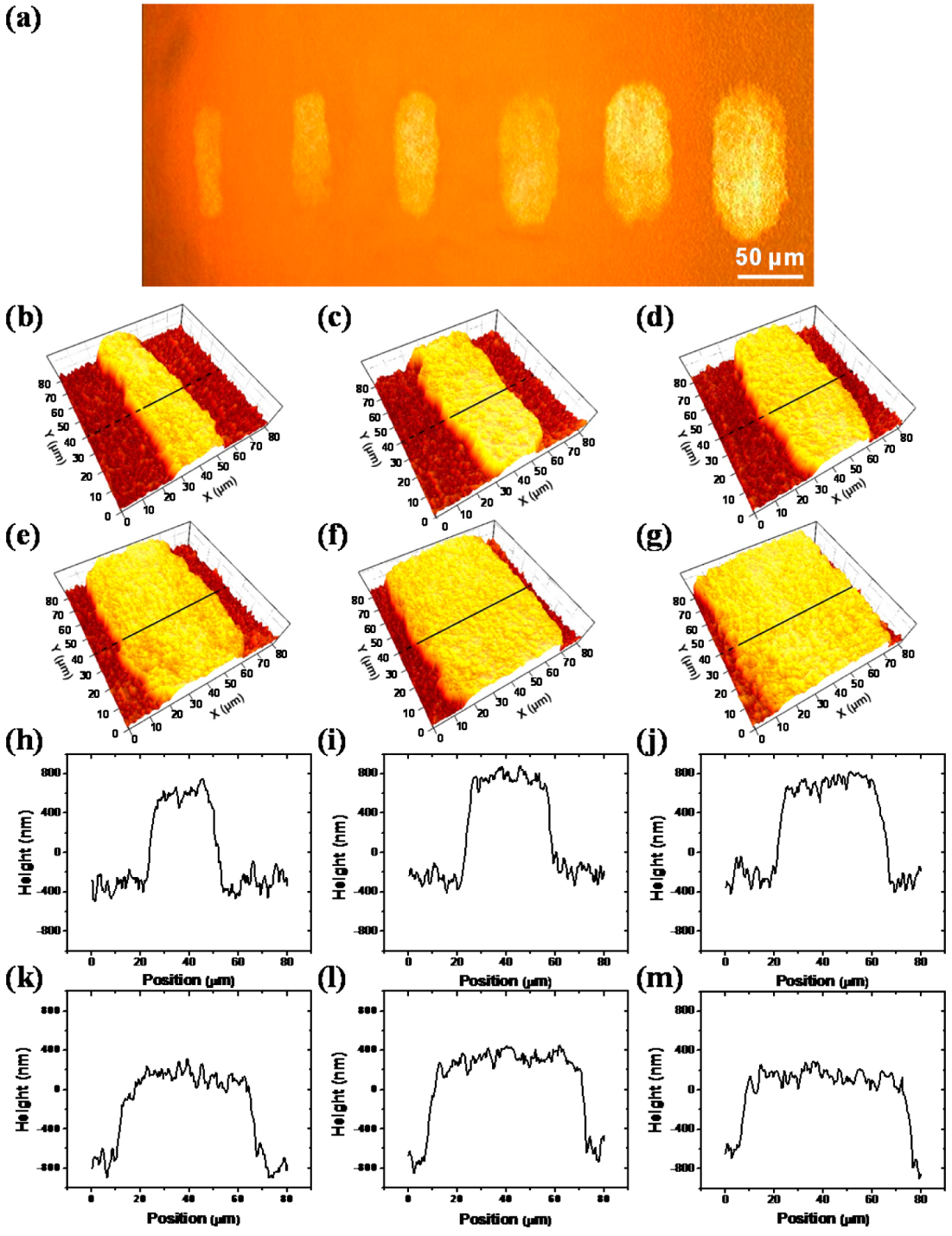

Figure 6. (a) Optical microscope image of microscopic lines written with increasing forces from left to right. (b–g) AFM images of the lines (from left to right) in (a). (h–m) Height profiles scanned across the dashed lines in (b)–(g).

Table 1. Dependence of the Recovered Line Widths on the Parameters of the AFM-Based Direct Writing Process

	set-point voltage (V)					
	0.005	0.01	0.05	0.1	0.3	0.5
writing force (μN)	13.8	27.7	138	277	830	1380
line width (μm)	25.8 ± 1.9	33.0 ± 2.7	40.4 ± 1.1	44.3 ± 1.6	53.8 ± 2.2	60.4 ± 1.1
contact pressure (kPa)	26.2	32.0	106.7	177.4	361.1	477.4

~1.2 μm. This means the SMP can recover to its permanent shape due to the tip–sample interaction, which is in part caused by the attractive force (adhesion) between the tip and the copolymer membrane.[30] This attractive force is contributed by both the van der Waals interactions and the capillary force generated by the water meniscus bridging between the tip and

DOI: 10.1021/acsami.5b07220
ACS Appl. Mater. Interfaces 2015, 7, 23650–23659

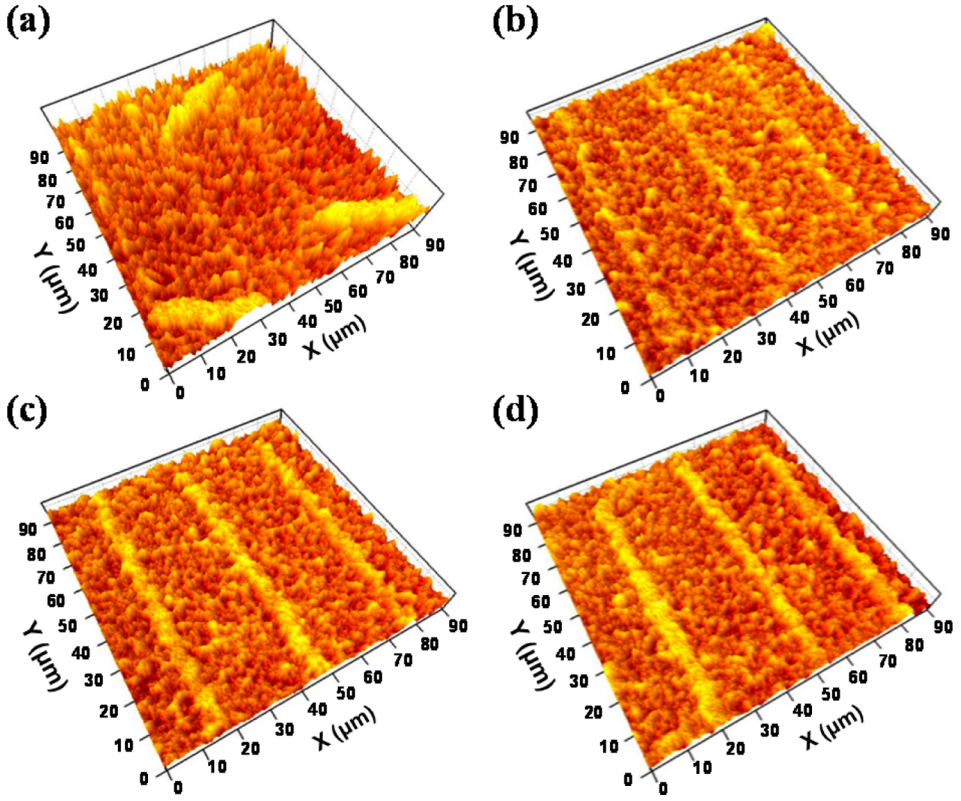

Figure 7. AFM images of nanoscopic lines written with different AFM tip speeds: (a) 0.2 μm/s; (b) 1 μm/s; (c) 5 μm/s; (d) 20 μm/s.

sample.[54] The average maximum attractive force (F_{attr}^{ave}) can be determined from the measurement of the pull-off force required to disengage the contact of the AFM tip with the sample. The contact force was calculated as the difference between the F_{attr}^{ave} and the pulling force applied by the tip. The minimum pressure that can induce the SM recovery was determined by $P_m = F_m/A$, where P_m is the minimum pressure, F_m is the minimum contact force, and $A = \pi r^2$ is the contact area. The minimum contact radius r is calculated as half of the line width. Table 1 summarizes the writing forces, the resulting line widths, and the calculated contact pressures. The minimum contact pressure that can cause the macropore recovery was determined to be ~26 kPa. Quasi-static indentation was also explored to compare with the dynamic direct writing process. However, even with an applied force 1000 times larger than the writing one, the SMP surface was barely recovered by quasi-static indentation, as there was no distinguishable diffractive photonic crystal pattern generated. The SM recovery mechanisms and the difference between these two processes will be discussed in section 3.6.

3.5. Writing Speed Effects on SM Recovery. To further investigate the writing speed effects on the SMP surface recovery, as well as the minimal line width enabled by AFM directly writing, a 20 μm diameter borosilicate spherical tip was used to perform a series of writing experiments. By use of a smaller tip radius, the resolution is significantly increased along with the sensitivity in writing speed. The AFM images in Figure 7 show nanoscopic lines written with the same force (6 μN), but the writing speed was increased from 0.2 μm/s (Figure 7a) to 20 μm/s (Figure 7d). The characteristics of the resulting nanopatterns including line widths and protruding heights are summarized in Table 2. It is apparent that both the line widths and heights of the recovered nanopatterns increased with higher writing speed. This set of experiments confirms that the SM recovery of the deformed macropores is dependent on the lateral motion and perturbation between the AFM tip and the SMP membrane.

Table 2. Dependence of the Recovered Line Width and Height on the Writing Speed of the AFM Tip

	writing speed (μm/s)			
	0.2	1	5	20
line width (μm)	4.1 ± 0.4	5.6 ± 0.9	6.0 ± 0.9	6.4 ± 0.4
line height (nm)	301 ± 12	407 ± 17	477 ± 20	526 ± 29

3.6. SM Recovery Mechanisms. All above experimental results have indicated that the direct writing approach is not a simple and straightforward extension of the static printing technology as reported in our previous work.[30] From an energy perspective, the SM deformation and recovery processes are due to the energy transformation between the external (i.e., capillary pressure induced by water evaporation, applied contact force, and shear stress caused by tip lateral motion) and the internal (e.g., polymer chain movement, internal energy change, and stored elastic energy) of the SMP system. At room temperature, the ETPTA 20-*co*-PEGDA 600 copolymer is in its rubbery state, above the glass transition temperature ($T_g \approx -42$ °C).[30] The polymer chains are highly compliant at room temperature, and the polymer behaves like a soft (viscous) elastic material.[55] The large capillary pressure induced by the high surface tension of water collapses the originally ordered macropores during the water evaporation process.[30] To reactivate the squeezed polymer chains and trigger the collapsed macropore recovery to its original configuration, external input energy is needed or, equivalently, a reverse process to water evaporation is needed. Mechanical stress, in the form of either statically or dynamically applied force by a rubber stamp or a writing tip, can input energy

DOI: 10.1021/acsami.5b07220
ACS Appl. Mater. Interfaces 2015, 7, 23650−23659

into the SMP system.[56] In the case of direct writing, the energy required to overcome the SM activation barrier is provided by sliding the tip across the SMP surface with a compressive force. The kinetic energy of the tip is transferred to the polymer matrix in the form of shear deformation and vibration.[56−58] The combination of shear and vibration, which increases the internal energy of the SMP system, provides the energy to activate polymer chain mobility and trigger the macropore recovery. Our experimental results show that with higher tip sliding speed, a more complete recovery of SMP was achieved, which was presented as a higher recovered line width and height (see Figure 7). This is in accordance with intuition that the more input energy, the higher is the density of activated polymer chains.

It has been argued that the shear stress field can induce changes in the conformation of intermolecular bonds and polymer chain flow in glassy polymers at temperatures above T_g.[59] In addition, a recent study was able to directly measure stress-induced molecular mobility in glassy polymers.[60] Mobility was shown to increase by 10- to 1000-fold after stress was applied. Furthermore, nanoscopically raised patterns were observed when a polyethylene oxide (PEO) film was raster-scanned by an AFM tip at ambient conditions.[58] Viscoelastic effects and localized heating caused by rupture of the adhesive bonds between the tip and the polymer, which could raise the local surface temperature by up to several hundred kelvin, were attributed to the unexpected formation of the raised areas during scanning. These studies support what we observed with the effects of the tip materials (e.g., LDPE vs stainless stain tip) and the varying writing speed (i.e., strain rate) on the SM macropore recovery. LDPE-wrapped tips, which could induce stronger van der Waals interactions with the ETPTA 20-*co*-PEGDA 600 copolymers than stainless steel tips, are thus more efficient in inducing a more complete SM recovery during direct writing. In the case of quasi-static indentation, only vertical contact between the tip and the SMP membrane was involved. During indentation, the AFM tip compressed the macroporous structure to a more squeezed configuration. The majority of the external energy was stored in the elastic deformation of the polymer matrix. Only very limited kinetic energy was transferred as internal energy to activate the polymer chains. As a result, a comparatively larger force is expected to reactivate the polymer chain mobility than in the dynamic writing case. In retraction, the stored elastic potential energy was gradually released as the SMP surface returned to its initial contact height. Then the attractive adhesion force between the tip and the sample acted as the subsequent recovery force.[30] Our experimental results support this conjecture. It is worthy to point out that the minimum force that can cause macropore recovery in quasi-static indentation is 2−3 orders magnitude higher than that in dynamic writing. Assuming the indention process is one extreme case in writing for which the lateral speed is zero, then it is clear that the dominant energy to induce SM recovery comes from the lateral movement of the writing tip.

4. CONCLUSIONS

By integrating the well-established templating nanofabrication with a new type of pressure-responsive SMP, we have developed a dynamic direct writing technology for fabricating 3D ordered macroporous photonic crystal patterns in a single step. We have demonstrated that both macroscopic and nanoscopic photonic crystal features can be reversibly patterned and erased, highly desirable for developing reconfigurable nanooptical devices. Systematic experiments have revealed the importance of the material selection, dimension, applied force, and writing speed of the tips in affecting the SM recovery of 3D ordered macropores. Importantly, the dynamic writing approach exhibits significant differences in SM recovery mechanisms and critical recovery force than quasi-static indentation. Besides straightforward applications in photonic crystal devices and nanooptics, the striking chromogenic effects induced by the disorder-to-order transition during SM recovery of ordered macropores, the manifest protrusion of the recovered regions, the sensitivity of the SMP membranes to various mechanical stresses, the unusual room-temperature operation for the entire shape-memory cycle (from programming to recovery), and the microscopic resolution of the directly written features could add new dimensions to many existing and future applications, such as in mechanochromic stress and impact sensors,[61−65] rewritable high-density optical data storage media,[66,67] chromogenic chemical sensors,[68,69] and tunable phononic crystals for controlling the flow of phonons.[49,70]

■ ASSOCIATED CONTENT

Supporting Information

The Supporting Information is available free of charge on the ACS Publications website at DOI: 10.1021/acsami.5b07220.

Optical reflection spectra of writing and erasing processes (PDF)

Video of direct writing of macroscopic photonic crystal patterns on macroporous SMP membrane using a LDPE-wrapped pencil (AVI)

Video of repeated erasing and rewriting of macroscopic photonic crystal patterns on macroporous SMP membranes using a LDPE-wrapped pencil (AVI)

■ AUTHOR INFORMATION

Corresponding Authors

*C.T.: e-mail, curtis.taylor@ufl.edu.

*P.J.: e-mail, pjiang@che.ufl.edu.

Author Contributions

‖Y.F. and Y.N. contributed equally.

The manuscript was written through contributions of all authors. All authors have given approval to the final version of the manuscript.

Notes

The authors declare no competing financial interest.

■ ACKNOWLEDGMENTS

This work was partially supported by the U.S. Defense Threat Reduction Agency, Basic Research Award HDTRA1-15-1-0022, to University of Florida and an Early Stage Innovations grant (Award NNX14AB07G) from NASA's Space Technology Research Grants Program. Acknowledgments are also made to the U.S. National Science Foundation (NSF) under Award CMMI-1300613 and Marie Curie IRSES Project 247614-NET4m.

■ REFERENCES

(1) Tumbleston, J. R.; Shirvanyants, D.; Ermoshkin, N.; Janusziewicz, R.; Johnson, A. R.; Kelly, D.; Chen, K.; Pinschmidt, R.; Rolland, J. P.; Ermoshkin, A.; Samulski, E. T.; DeSimone, J. M. Continuous Liquid Interface Production of 3d Objects. *Science* **2015**, *347*, 1349−1352.

(2) Li, J.; He, L.; Zhou, C.; Zhou, Y.; Bai, Y.; Lee, F. Y.; Mao, J. J. 3d Printing for Regenerative Medicine: From Bench to Bedside. *MRS Bull.* **2015**, *40*, 145−153.

DOI: 10.1021/acsami.5b07220
ACS Appl. Mater. Interfaces 2015, 7, 23650−23659

(3) Gross, B. C.; Erkal, J. L.; Lockwood, S. Y.; Chen, C.; Spence, D. M. Evaluation of 3d Printing and Its Potential Impact on Biotechnology and the Chemical Sciences. *Anal. Chem.* **2014**, *86*, 3240−3253.
(4) Lewis, J. A. Direct Ink Writing of 3d Functional Materials. *Adv. Funct. Mater.* **2006**, *16*, 2193−2204.
(5) Sun, K.; Wei, T.-S.; Ahn, B. Y.; Seo, J. Y.; Dillon, S. J.; Lewis, J. A. 3d Printing of Interdigitated Li-Ion Microbattery Architectures. *Adv. Mater.* **2013**, *25*, 4539−4543.
(6) Lessing, J.; Glavan, A. C.; Walker, S. B.; Keplinger, C.; Lewis, J. A.; Whitesides, G. M. Inkjet Printing of Conductive Inks with High Lateral Resolution on Omniphobic "R-F Paper" for Paper-Based Electronics and MEMS. *Adv. Mater.* **2014**, *26*, 4677−4682.
(7) Murphy, S. V.; Atala, A. 3d Bioprinting of Tissues and Organs. *Nat. Biotechnol.* **2014**, *32*, 773−785.
(8) Rinne, S. A.; Garcia-Santamaria, F.; Braun, P. V. Embedded Cavities and Waveguides in Three-Dimensional Silicon Photonic Crystals. *Nat. Photonics* **2008**, *2*, 52−56.
(9) Gratson, G. M.; Garcia-Santamaria, F.; Lousse, V.; Xu, M. J.; Fan, S. H.; Lewis, J. A.; Braun, P. V. Direct-Write Assembly of Three-Dimensional Photonic Crystals: Conversion of Polymer Scaffolds to Silicon Hollow-Woodpile Structures. *Adv. Mater.* **2006**, *18*, 461−465.
(10) Shen, W.; Li, M.; Ye, C.; Jiang, L.; Song, Y. Direct-Writing Colloidal Photonic Crystal Microfluidic Chips by Inkjet Printing for Label-Free Protein Detection. *Lab Chip* **2012**, *12*, 3089−3095.
(11) Froelich, A.; Fischer, J.; Zebrowski, T.; Busch, K.; Wegener, M. Titania Woodpiles with Complete Three-Dimensional Photonic Bandgaps in the Visible. *Adv. Mater.* **2013**, *25*, 3588−3592.
(12) Thiel, M.; Fischer, J.; von Freymann, G.; Wegener, M. Direct Laser Writing of Three-Dimensional Submicron Structures Using a Continuous-Wave Laser at 532 Nm. *Appl. Phys. Lett.* **2010**, *97*, 221102.
(13) Lenhert, S.; Brinkmann, F.; Laue, T.; Walheim, S.; Vannahme, C.; Klinkhammer, S.; Xu, M.; Sekula, S.; Mappes, T.; Schimmel, T.; Fuchs, H. Lipid Multilayer Gratings. *Nat. Nanotechnol.* **2010**, *5*, 275−279.
(14) Lee, W. M.; Pruzinsky, S. A.; Braun, P. V. Multi-Photon Polymerization of Waveguide Structures within Three-Dimensional Photonic Crystals. *Adv. Mater.* **2002**, *14*, 271−274.
(15) Joannopoulos, J. D.; Meade, R. D.; Winn, J. N. *Photonic Crystals: Molding the Flow of Light*; Princeton University Press: Princeton, NJ, 1995.
(16) Grillet, C.; Monat, C.; Smith, C. L.; Lee, M. W.; Tomljenovic-Hanic, S.; Karnutsch, C.; Eggleton, B. J. Reconfigurable Photonic Crystal Circuits. *Laser Photonics Rev.* **2010**, *4*, 192−204.
(17) Ge, J. P.; Yin, Y. D. Magnetically Responsive Colloidal Photonic Crystals. *J. Mater. Chem.* **2008**, *18*, 5041−5045.
(18) Zhang, J.; Li, Y.; Zhang, X.; Yang, B. Colloidal Self-Assembly Meets Nanofabrication: From Two-Dimensional Colloidal Crystals to Nanostructure Arrays. *Adv. Mater.* **2010**, *22*, 4249−4269.
(19) Velev, O. D.; Jede, T. A.; Lobo, R. F.; Lenhoff, A. M. Porous Silica Via Colloidal Crystallization. *Nature* **1997**, *389*, 447−448.
(20) Hatton, B.; Mishchenko, L.; Davis, S.; Sandhage, K. H.; Aizenberg, J. Assembly of Large-Area, Highly Ordered, Crack-Free Inverse Opal Films. *Proc. Natl. Acad. Sci. U. S. A.* **2010**, *107*, 10354−10359.
(21) Lendlein, A. *Shape Memory Polymers*; Springer: New York, NY, 2010.
(22) Mather, P. T.; Luo, X.; Rousseau, I. A. Shape Memory Polymer Research. *Annu. Rev. Mater. Res.* **2009**, *39*, 445−471.
(23) Xie, T.; Xiao, X.; Li, J.; Wang, R. Encoding Localized Strain History through Wrinkle Based Structural Colors. *Adv. Mater.* **2010**, *22*, 4390−4394.
(24) Arsenault, A. C.; Puzzo, D. P.; Manners, I.; Ozin, G. A. Photonic-Crystal Full-Colour Displays. *Nat. Photonics* **2007**, *1*, 468−472.
(25) Vlasov, Y. A.; Bo, X. Z.; Sturm, J. C.; Norris, D. J. On-Chip Natural Assembly of Silicon Photonic Bandgap Crystals. *Nature* **2001**, *414*, 289−293.
(26) Wijnhoven, J.; Vos, W. L. Preparation of Photonic Crystals Made of Air Spheres in Titania. *Science* **1998**, *281*, 802−804.
(27) Kuncicky, D. M.; Prevo, B. G.; Velev, O. D. Controlled Assembly of Sers Substrates Templated by Colloidal Crystal Films. *J. Mater. Chem.* **2006**, *16*, 1207−1211.
(28) Fu, M.; Chaudhary, K.; Lange, J. G.; Kim, H. S.; Juarez, J. J.; Lewis, J. A.; Braun, P. V. Anisotropic Colloidal Templating of 3d Ceramic, Semiconducting, Metallic, and Polymeric Architectures. *Adv. Mater.* **2014**, *26*, 1740−1745.
(29) Hou, J.; Zhang, H.; Yang, Q.; Li, M.; Jiang, L.; Song, Y. Hydrophilic-Hydrophobic Patterned Molecularly Imprinted Photonic Crystal Sensors for High-Sensitive Colorimetric Detection of Tetracycline. *Small* **2015**, *11*, 2738−2742.
(30) Fang, Y.; Ni, Y.; Leo, S.-Y.; Taylor, C.; Basile, V.; Jiang, P. Reconfigurable Photonic Crystals Enabled by Pressure-Responsive Shape-Memory Polymers. *Nat. Commun.* **2015**, *6*, 7416.
(31) Fang, Y.; Ni, Y.; Choi, B.; Leo, S.-Y.; Gao, J.; Ge, B.; Taylor, C.; Basile, V.; Jiang, P. Chromogenic Photonic Crystals Enabled by Novel Vapor-Responsive Shape-Memory Polymers. *Adv. Mater.* **2015**, *27*, 3696−3704.
(32) Lendlein, A.; Jiang, H. Y.; Junger, O.; Langer, R. Light-Induced Shape-Memory Polymers. *Nature* **2005**, *434*, 879−882.
(33) Lendlein, A.; Kelch, S. Shape-Memory Polymers. *Angew. Chem., Int. Ed.* **2002**, *41*, 2034−2057.
(34) Behl, M.; Razzaq, M. Y.; Lendlein, A. Multifunctional Shape-Memory Polymers. *Adv. Mater.* **2010**, *22*, 3388−3410.
(35) Xie, T. Recent Advances in Polymer Shape Memory. *Polymer* **2011**, *52*, 4985−5000.
(36) Gu, X.; Mather, P. T. Water-Triggered Shape Memory of Multiblock Thermoplastic Polyurethanes (TPUS). *RSC Adv.* **2013**, *3*, 15783−15791.
(37) Zhang, H.; Zhao, Y. Polymers with Dual Light-Triggered Functions of Shape Memory and Healing Using Gold Nanoparticles. *ACS Appl. Mater. Interfaces* **2013**, *5*, 13069−13075.
(38) Kuroki, H.; Islam, C.; Tokarev, I.; Hu, H.; Liu, G.; Minko, S. Tunable Ultrathin Membranes with Nonvolatile Pore Shape Memory. *ACS Appl. Mater. Interfaces* **2015**, *7*, 10401−10406.
(39) Xie, T. Tunable Polymer Multi-Shape Memory Effect. *Nature* **2010**, *464*, 267−270.
(40) Huang, W. M.; Yang, B.; Fu, Y. Q. *Polyurethane Shape Memory Polymers*; CRC Press: Boca Raton, FL, 2012.
(41) Meng, H.; Hu, J. A Brief Review of Stimulus-Active Polymers Responsive to Thermal, Light, Magnetic, Electric, and Water/Solvent Stimuli. *J. Intell. Mater. Syst. Struct.* **2010**, *21*, 859−885.
(42) Tippets, C. A.; Li, Q.; Fu, Y.; Donev, E. U.; Zhou, J.; Turner, S. A.; Jackson, A.-M. S.; Ashby, V. S.; Sheiko, S. S.; Lopez, R. Dynamic Optical Gratings Accessed by Reversible Shape Memory. *ACS Appl. Mater. Interfaces* **2015**, *7*, 14288−93.
(43) Espinha, A.; Concepcion Serrano, M.; Blanco, A.; Lopez, C. Thermoresponsive Shape-Memory Photonic Nanostructures. *Adv. Opt. Mater.* **2014**, *2*, 516−521.
(44) Turner, S. A.; Zhou, J.; Sheiko, S. S.; Ashby, V. S. Switchable Micropatterned Surface Topographies Mediated by Reversible Shape Memory. *ACS Appl. Mater. Interfaces* **2014**, *6*, 8017−8021.
(45) Xu, H.; Yu, C.; Wang, S.; Malyarchuk, V.; Xie, T.; Rogers, J. A. Deformable, Programmable, and Shape-Memorizing Micro-Optics. *Adv. Funct. Mater.* **2013**, *23*, 3299−3306.
(46) Wang, Z.; Hansen, C.; Ge, Q.; Maruf, S. H.; Ahn, D. U.; Qi, H. J.; Ding, Y. Programmable, Pattern-Memorizing Polymer Surface. *Adv. Mater.* **2011**, *23*, 3669−3673.
(47) Schaefer, C. G.; Gallei, M.; Zahn, J. T.; Engelhardt, J.; Hellmann, G. P.; Rehahn, M. Reversible Light-, Thermo-, and Mechano-Responsive Elastomeric Polymer Opal Films. *Chem. Mater.* **2013**, *25*, 2309−2318.
(48) Schaefer, C. G.; Smolin, D. A.; Hellmann, G. P.; Gallei, M. Fully Reversible Shape Transition of Soft Spheres in Elastomeric Polymer Opal Films. *Langmuir* **2013**, *29*, 11275−11283.
(49) Jang, J.-H.; Koh, C. Y.; Bertoldi, K.; Boyce, M. C.; Thomas, E. L. Combining Pattern Instability and Shape-Memory Hysteresis for Phononic Switching. *Nano Lett.* **2009**, *9*, 2113−2119.

DOI: 10.1021/acsami.5b07220
ACS Appl. Mater. Interfaces 2015, 7, 23650−23659

(50) Stober, W.; Fink, A.; Bohn, E. Controlled Growth of Monodisperse Silica Spheres in Micron Size Range. *J. Colloid Interface Sci.* **1968**, *26*, 62−69.
(51) Jiang, P.; Bertone, J. F.; Hwang, K. S.; Colvin, V. L. Single-Crystal Colloidal Multilayers of Controlled Thickness. *Chem. Mater.* **1999**, *11*, 2132−2140.
(52) Satpathy, S.; Zhang, Z.; Salehpour, M. R. Theory of Photon Bands in 3-Dimensional Periodic Dielectric Structures. *Phys. Rev. Lett.* **1990**, *64*, 1239−1242.
(53) Jiang, P.; Hwang, K. S.; Mittleman, D. M.; Bertone, J. F.; Colvin, V. L. Template-Directed Preparation of Macroporous Polymers with Oriented and Crystalline Arrays of Voids. *J. Am. Chem. Soc.* **1999**, *121*, 11630−11637.
(54) Butt, H. J.; Cappella, B.; Kappl, M. Force Measurements with the Atomic Force Microscope: Technique, Interpretation and Applications. *Surf. Sci. Rep.* **2005**, *59*, 1−152.
(55) Odian, G. *Principles of Polymerization*, 3rd ed.; John Wiley & Sons: Staten Island, NY, 1991.
(56) Xie, X. N.; Chung, H. J.; Sow, C. H.; Wee, A. T. S. Nanoscale Materials Patterning and Engineering by Atomic Force Microscopy Nanolithography. *Mater. Sci. Eng., R* **2006**, *54*, 1−48.
(57) Nie, H. Y.; Motomatsu, M.; Mizutani, W.; Tokumoto, H. Local Modification of Elastic Properties of Polystyrene-Polyethyleneoxide Blend Surfaces. *J. Vac. Sci. Technol., B: Microelectron. Process. Phenom.* **1995**, *13*, 1163−1166.
(58) Jin, X.; Unertl, W. N. Submicrometer Modification of Polymer Surfaces with a Surface Force Microscope. *Appl. Phys. Lett.* **1992**, *61*, 657−659.
(59) Robertson, R. E. Theory for Plasticity of Glassy Polymers. *J. Chem. Phys.* **1966**, *44*, 3950−3956.
(60) Lee, H.-N.; Paeng, K.; Swallen, S. F.; Ediger, M. D. Direct Measurement of Molecular Mobility in Actively Deformed Polymer Glasses. *Science* **2009**, *323*, 231−234.
(61) Lee, K. J.; Yoon, J.; Rahmani, S.; Hwang, S.; Bhaskar, S.; Mitragotri, S.; Lahann, J. Spontaneous Shape Reconfigurations in Multicompartmental Microcylinders. *Proc. Natl. Acad. Sci. U. S. A.* **2012**, *109*, 16057−16062.
(62) Lee, J. H.; Veysset, D.; Singer, J. P.; Retsch, M.; Saini, G.; Pezeril, T.; Nelson, K. A.; Thomas, E. L. High Strain Rate Deformation of Layered Nanocomposites. *Nat. Commun.* **2012**, *3*, 1164.
(63) He, L.; Janner, M.; Lu, Q.; Wang, M.; Ma, H.; Yin, Y. Magnetochromatic Thin-Film Microplates. *Adv. Mater.* **2015**, *27*, 86−92.
(64) Yang, D.; Ye, S.; Ge, J. From Metastable Colloidal Crystalline Arrays to Fast Responsive Mechanochromic Photonic Gels: An Organic Gel for Deformation-Based Display Panels. *Adv. Funct. Mater.* **2014**, *24*, 3197−3205.
(65) Fudouzi, H.; Sawada, T. Photonic Rubber Sheets with Tunable Color by Elastic Deformation. *Langmuir* **2006**, *22*, 1365−1368.
(66) Altebaeumer, T.; Gotsmann, B.; Pozidis, H.; Knoll, A.; Duerig, U. Nanoscale Shape-Memory Function in Highly Cross-Linked Polymers. *Nano Lett.* **2008**, *8*, 4398−4403.
(67) Hu, Z.; Tian, M.; Nysten, B.; Jonas, A. M. Regular Arrays of Highly Ordered Ferroelectric Polymer Nanostructures for Non-Volatile Low-Voltage Memories. *Nat. Mater.* **2009**, *8*, 62−67.
(68) Zhang, Y. Q.; Fu, Q. Q.; Ge, J. P. Photonic Sensing of Organic Solvents through Geometric Study of Dynamic Reflection Spectrum. *Nat. Commun.* **2015**, *6*, 7510.
(69) Wang, H.; Zhang, K.-Q. Photonic Crystal Structures with Tunable Structure Color as Colorimetric Sensors. *Sensors* **2013**, *13*, 4192−4213.
(70) Lee, J.-H.; Koh, C. Y.; Singer, J. P.; Jeon, S.-J.; Maldovan, M.; Stein, O.; Thomas, E. L. 25th Anniversary Article: Ordered Polymer Structures for the Engineering of Photons and Phonons. *Adv. Mater.* **2014**, *26*, 532−568.

DOI: 10.1021/acsami.5b07220
ACS Appl. Mater. Interfaces 2015, 7, 23650−23659